

SYNTHESIS OF MESO- AND MACROPOROUS CARBON AEROGELS

Liviu Cosmin COTEȚ,^a Virginia DANCIU,^{*a} Veronica COȘOVEANU,^a Ionel Cătălin POPESCU,^a Anna ROIG^b and Elies MOLINS^b

^aFaculty of Chemistry and Chemical Engineering, Babes-Bolyai University, 11 Arany Janos str., 400028 Cluj-Napoca, Roumania

^bInstitut de Ciència de Materials de Barcelona (ICMAB-CSIC), Campus Universitat Autònoma de Barcelona (UAB), 08193 Bellaterra, Catalunya, Spain

Received June 7, 2006

Organic and carbon aerogels with of meso- and/or macroporosity were obtained by sol-gel using different precursor/catalyst and precursor/water molar ratios. By polycondensation of resorcinol (R) and formaldehyde (F), wet resorcinol-formaldehyde (RF) gels were prepared. Using CO₂ supercritical drying, the RF gels were transformed into organic aerogels and to carbon aerogels by pyrolysis under nitrogen atmosphere. The monolith organic and carbon aerogels were investigated by BET, TEM, AFM, SEM and XRD techniques. When using R/C ≤ 100, mesoporous carbon aerogels with high BET surface area from 800 to 1100 m²/g were obtained, whereas for R/C > 100, the resulting carbon aerogels were mostly macroporous. Moreover, in the case of R/C=1500, graphitic pseudo crystalline forms were identified in the carbon aerogels.

INTRODUCTION

Carbon aerogels are very interesting monolithic materials with a large spectrum of potential applications resulting from some of their properties: low electrical resistivity, high surface area, high open porosity and controllable morpho-structural characteristics.¹⁻⁴ The synthesis of this material is usually based on the polycondensation of resorcinol with formaldehyde using Na₂CO₃ as catalyst (C). Supercritical drying of RF gels followed by a pyrolysis treatment usually gives rise to mesoporous carbon aerogels.^{5,6}

In order to obtain carbon aerogels with controllable meso/macro porosity, a wide range of resorcinol/catalyst (R/C) and resorcinol/water (R/W) ratios were used (see Table 1). The morpho-structural characteristics of the organic and carbon aerogels thus obtained were investigated by means of the N₂ adsorption (BET method), transmission electron microscopy (TEM), atomic force microscopy (AFM), scanning electron microscopy (SEM) and X-ray diffraction (XRD).

Table 1

Synthesis parameters (R/C and R/W ratios), bulk density and BET surface area for resorcinol-formaldehyde (RFA) and carbon (CA) aerogels*

Sample	R/C [mol/mol]	R/W [g/cm ³]	Density [g/cm ³]		S _{BET} [m ² /g]	
			RFA (±0,01)	CA (±0,01)	RFA (±30)	CA (±30)
“sA”	50	0,032	0,16	0,27	600	1096
“sB”	76,3	0,032	0,10	0,21	520	1126
“sC”	96,6	0,032	0,08	0,17	617	820
“sD”	200	0,032	0,03	0,08	520	849
“sE”	400	0,032	0,05	0,06	309	782
“sF”	600	0,032	0,04	0,06	177	591
“sG”	800	0,032	0,13	0,08	140	697
“sH”	1000	0,077	0,11	0,12	128	540
“sI”	1500	0,200	0,26	0,24	84	160

* Author correspondent e-mail address: vdanciu@chem.ubbcluj.ro

RESULTS AND DISCUSSION

Carbon aerogels, as well as other oxide based aerogels, consist of interconnected nano-particles.⁵ Generally, the size of these particles is strongly dependent on the synthesis parameters: reactant ratios (R/C, R/W), pH of the reactant mixture (being the optimum range, 5.5-8) and the drying and pyrolysis conditions.¹

Thus, the samples prepared with high amount of catalyst (R/C < 100) reveal adsorption isotherms

with a hysteretic loops of type IV (Figure 1.a) and a Gaussian pore diameter distribution (Figure 2.a), typically associated to “inkbottle” shape mesopores (2-50 nm diameter). In this case, during the adsorption process, capillarity condensation is occurring. The samples prepared with R/C > 100 have adsorption isotherms with small loops (Figure 1.b) and a non-Gaussian pore diameter distribution (Figure 2.b). These characteristics are specifically for macroporous materials with larger and loosely connected particles.

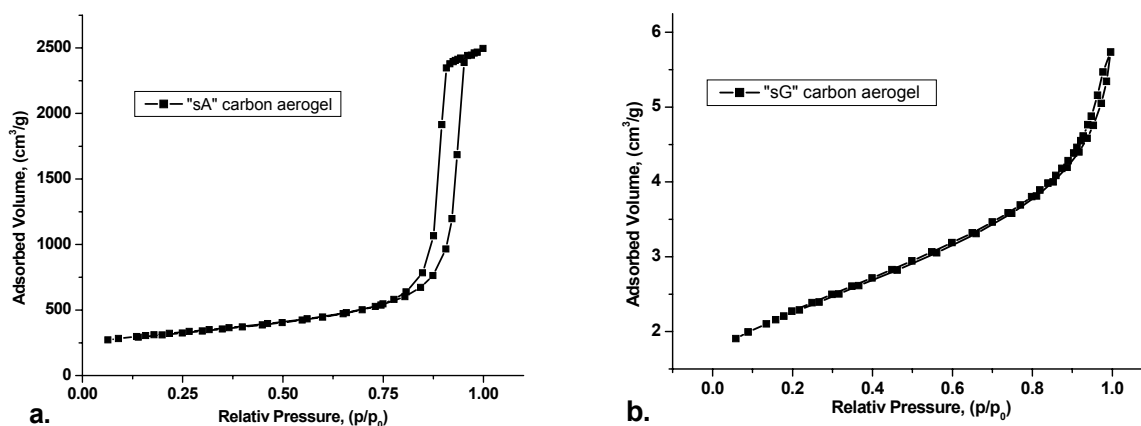


Fig. 1 – Adsorption-desorption isotherms of N₂ on the “sA”(a) and “sG”(b) carbon aerogels.

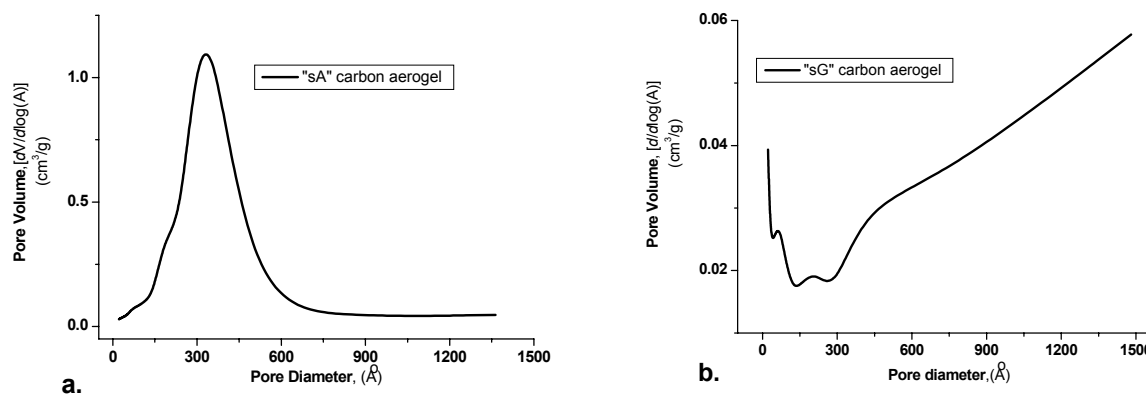


Fig. 2 – Pore size distribution of the “sA”(a) and “sG”(b) carbon aerogels.

The BET analyses reveal that all the samples have surface areas in the range of 200-1100 m²/g (see Table 1). As a general trend, the decreasing of the catalyst content gives rise to lighter aerogels with lower specific surface areas. It is noticeable that the carbon aerogels prepared with R/C = 76.3 present the highest BET (1126 m²/g) surface area. The increase of S_{BET} with decreasing R/C can be explained. It has been reported that RF aquagels, prepared under the conditions of low R/C, shrink greatly during supercritical drying.⁷ Thus, it is supposed that S_{BET} is small for lower R/C because

of the drying shrinkage followed by the collapse of aquagel structure. Consequently, the maximum value of S_{BET} is determined by the balance of the decrease of particle size of aquagels and the drying shrinkage.

The figures 3, 4 and 5, show SEM, TEM, and AFM images of three representative carbon aerogels, sC, sH and sI. The carbon particle size ranges from 5 to 3000 nm. As can be easily seen, for those samples prepared with lower catalyst amounts (higher R/C and R/W), the carbon nanoparticles forming the carbon aerogel

framework are larger. The lower catalyst amount determines the existence a few nucleation sites which favors the size carbon particle increasing in

the branching detriment. These phenomena explain “the pearl necklace” feature of these macroporous carbon aerogels (Figure 3.c).

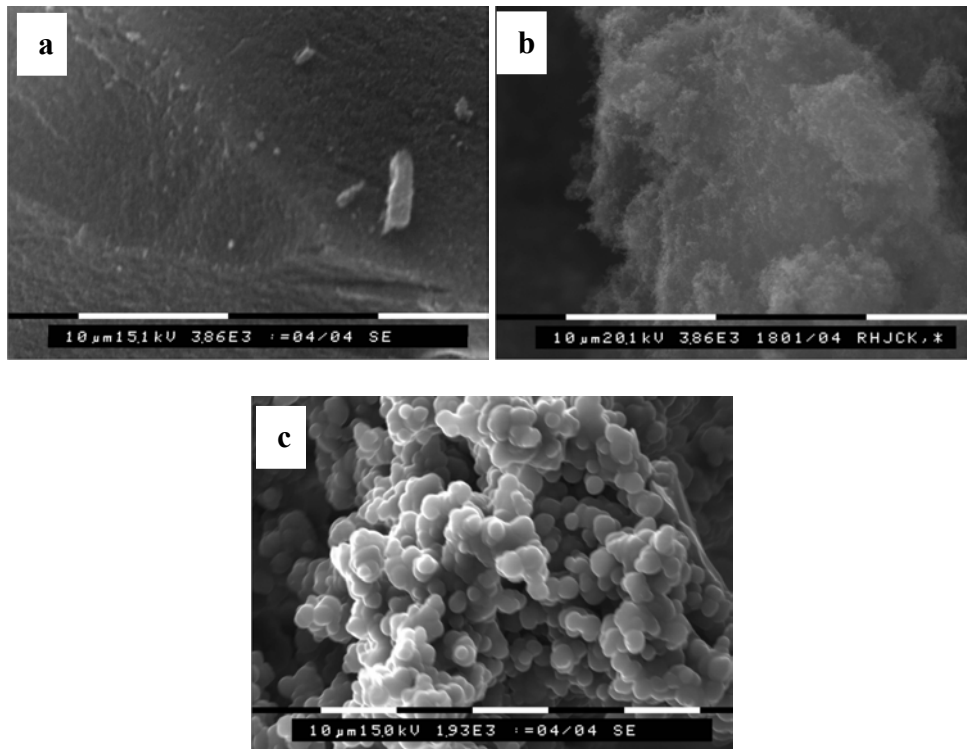


Fig. 3 – SEM images of the “sC” (a), “sH” (b), “sI” (c) carbon aerogels samples.

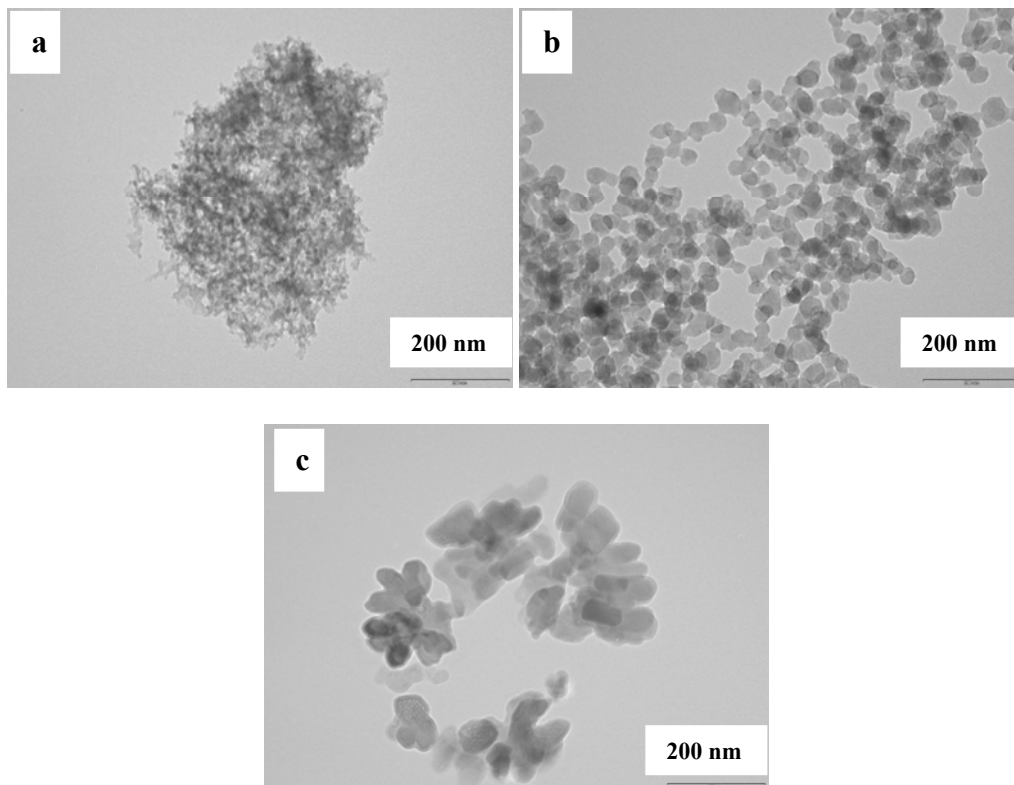


Fig. 4 – TEM images of the “sC” (a), “sH” (b), “sI” (c) carbon aerogels samples.

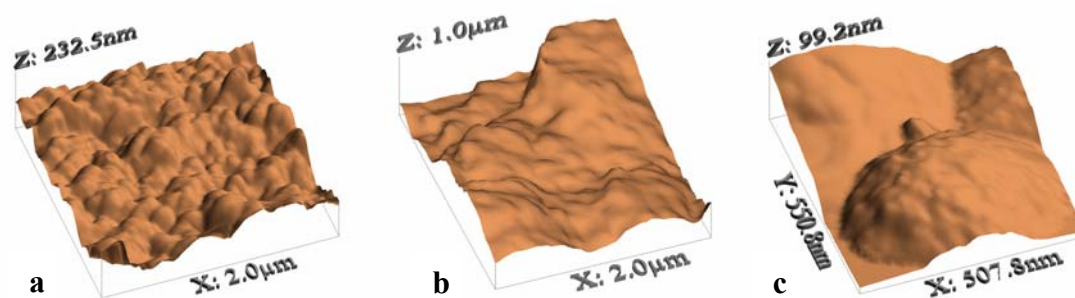


Fig. 5 – AFM images of the “sC” (a), “sH” (b), “sI” (c) carbon aerogels samples.

The X-ray diffraction analysis shows an amorphous structure both for the organic aerogels and the carbon aerogels. XRD patterns present two large peaks at about $2\theta = 24^\circ$ and 44° (Figure 6). However, in the case of “sI” carbon aerogel (see

Table 1), some pseudo graphitic forms are visualized - using the zonal electron diffraction (Figure 7). It has previously been observed that the degree of graphitization of carbon aerogels can be increased by their metal doping.⁸⁻¹²

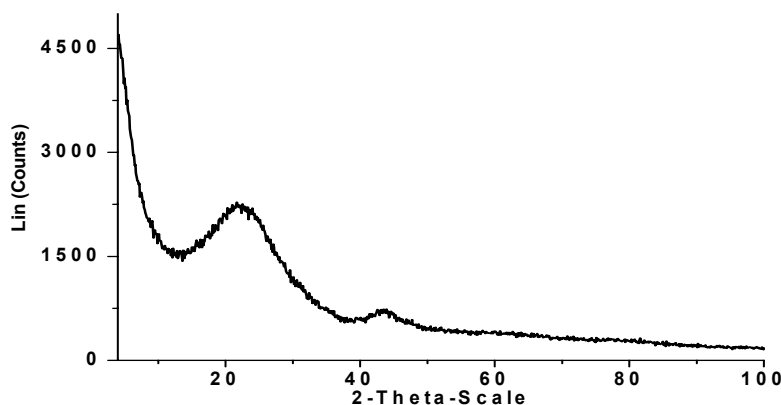


Fig. 6 – XRD patterns of the carbon aerogels.

Fig. 7 – Zonal electron diffraction of the “sI” carbon aerogel sample.



The nanofibrous features of mesoporous carbon aerogels, synthesized with $R/C \leq 100$, are evidenced by means of TEM (Figure 4.a) and AFM (Figure 5.a) analysis. Figures 3c and 4c confirm the macroporous structure formed by interconnected aggregates of nanoparticles and observed by BET analysis.

After the gel drying and pyrolysis of the organic mesoporous aerogels, a higher shrinkage was observed. This is the reason of the increase of

their bulk density comparatively with the respective RF aerogels. The preponderant presence of the macropores determines the shrinkage decreasing. For this reason, the bulk density of the organic and carbon aerogels is practically the same, the low observed differences being in the error limits. On the other hand, during the pyrolysis, the mesoporosity increases and, consequently, the surface area of the carbon aerogels thus obtained is larger (see Table 1).

EXPERIMENTAL

1. Sample Preparation

The resorcinol-formaldehyde wet gels were prepared using resorcinol (98 % purity), formaldehyde (37 % solution), Na₂CO₃ (99.9 % purity), all from Aldrich, and deionized water. Resorcinol (0.29 moles) was dissolved in deionized water at a certain R/W ratio (see Table 1). Solution of formaldehyde was added to the resorcinol solution (R/F = 0.5) in vigorous stirring. Afterwards, Na₂CO₃ in 0.1 M aqueous solution was added to the previous mixture. The solutions were placed into tightly closed glass moulds (7 cm-length x 1 cm internal diameter) and cured: 1 day at room temperature, 1 day at 50°C and 3 days at 70°C. The resulting resorcinol-formaldehyde gels were washed with ethanol and dried with CO₂ in supercritical conditions (38-40°C, 90-100 atm) resulting in resorcinol-formaldehyde aerogels. The organic aerogels were pyrolysed in N₂ atmosphere for 4 hours, either at 850°C for the R/C < 100 samples or at 1050°C for the R/C > 100 samples, resulting in carbon aerogels.

2. Morpho-structural characterization

Surface area, pore size distribution and pore volume determinations were performed by the Brunauer-Emmett-Teller (BET) and Barret-Joyner-Halenda (BJH) methods using an ASAP 2000 surface area analyzer (Micrometrics Instruments Corp.). About 0.03g of sample was heated under vacuum (10⁻⁵ torr) to 110°C (for organic aerogels) and 130°C (for carbon aerogels) for at least 20 hours to remove all adsorbed species. The bulk densities of the samples were estimated by measuring the dimensions and the mass of each monolithic sample (Table 1). Transmission electron microscopy on the carbon aerogels was performed with a Hitachi H-7000 microscope operating at 125 keV. Scanning electron microscopy was performed with a Phillips SEM 515 microscope. The X-ray diffraction patterns were recorded in a θ -2 θ Bragg-Bretano geometry with a Siemens D5000 powder diffractometer with Cu-K α incident radiation ($\lambda=1.5406$ Å). AFM images were performed with PicoSPM from "Molecular Imaging".

CONCLUSIONS

By varying the synthesis parameters (R/C and R/W ratios) carbon aerogels with tuned porosity

were obtained. At resorcinol/catalyst molar ratios lower than 100 mesoporous carbon aerogels presenting high surface area (800-1100 m²/g) were attained, while the resulting carbon aerogels were macroporous when using resorcinol/catalyst molar ratio larger than 1000 and high water content. Moreover, carbon aerogels obtained with R/C =1500 present graphitic features. Research is in progress on assessing the use of macroporous carbon aerogels as material substrate for (bio)sensors.

REFERENCES

1. S. A. Al-Muhtaseb and J. A. Ritter, *Adv. Mater.*, **2003**, *15*, 101-114.
2. C. Schmitt, H. Probstle and J. Fricke, *J. Non-Crist. Solids*, **2001**, *285*, 277-282
3. S. J. Kim, S. W. Hwang and S. H. Hyun, *J. Mat. Sci.*, **2005**, *40*, 725-731
4. B. Fang, Y. -Z. Wei, K. Maruyama and M. Kumagai, *J. App. Electroch.* **2005**, *35*, 229-233
5. R. W. Pekala, *US Pat.*, 4,873,218, **1988**.
6. V. Danciu, L. C. Coteț, V. Coșoveanu and P. Mărginean, *Studia Univ. Babeș-Bolyai, Chemia*, **2003**, *XLVIII*, 185-192.
7. H. Tamon, H. Ishizaka, M. Mikami, M. Okazaki, *Carbon*, **1997**, *6*, 791-796
8. T. F. Baumann, G. A. Fox, J. H. Satcher, N. Yoshizawa, R. Fu and M. S. Dresselhaus, *Langmuir*, **2002**, *18*, 7073-7076.
9. R. Fu, T. F. Baumann, S. Cronin, G. Dresselhaus, M. S. Dresselhaus and J. H. Satcher, *Langmuir*, **2005**, *21*, 2647-2651.
10. C. Moreno-Castilla, F. J. Maldonado-Hodar, *Carbon*, **2005**, *43*, 455-465.
11. S. Martínez, A. Vallibera, L. C. Coteț, M. Popovici, L. Martín, A. Roig, M. Moreno Mañas and E. Molins, *New J. Chem.*, **2005**, *29*, 1342-1345
12. L. C. Coteț, M. Baia, L. Baia, I. C. Popescu, V. Coșoveanu, E. Indrea, J. Papp and V. Danciu, *J. Alloy. Compd.*, in press.

